An Universal Multi-Additive Strategy to Enhance Efficiency and Stability in Inverted Perovskite Solar Cells

Luigi Angelo Castriotta[1,#], Emanuele Calabrò[1,2,#], Francesco Di Giacomo[1,*], Sathy Harshavardhan Reddy[1], Daimiota Takhellambam[1], Barbara Paci[3], Amanda Generosi[3], Luca Serenelli[4], Francesca Menchini[4], Luca Martini[4], Mario Tucci[4], Aldo Di Carlo[1,3,*]

[1]CHOSE (Centre for Hybrid and Organic Solar Energy), Department of Electronic Engineering, University of Rome "Tor Vergata", 00133, Rome, Italy

[2]Greatcell Italy, Greatcell Solar Italia, Viale Castro Pretorio 122, Rome, 00185, Italy

[3]ISM-CNR, Istituto di Struttura della Materia, Consiglio Nazionale delle Ricerche, Roma, 00133, Italy

[4]ENEA, Casaccia Research Center, Via Anguillarese 301, Rome, 00123, Italy

[#]These authors contributed equally

[*]Corresponding Author: francesco.di.giacomo@uniroma2.it, aldo.dicarlo@uniroma2.it

Abstract

Perovskite solar technology has become a trend topic in the last decade, reaching promising efficiencies up to 25.7%. Researchers mainly focused on obtaining high performances rather than caring for stability under accelerated stress condition, such as thermal and light soaking tests. For this reason, we studied a standard triple cation perovskite (~1.58eV) and wider bandgap perovskite (~1.63eV) with the scope of finding a common strategy to build a robust device stable over time independently of the perovskite used. We use a combination of additives inside the perovskite ink: ionic liquids 1-Butyl-3-methylimidazolium tetrafluoroborate (BMIM-BF4), alkylamine ligands oleylamine (OAm) and benzylhydrazine hydrochloride (BHC). Our work reveals that the combination of these additives helps to improve efficiency and stability of the entire device, reaching a power conversion efficiency of over 20% on both types of perovskite and stability beyond 1000 hours under continuous light-soaking. The universal applicability of this method further applied to a more robust methylammonium free perovskite leading to an impressive stability both under light soaking and under 85°C, showing T_{90} > 1500 hours and T_{80} > 8658 hours, respectively.

Introduction

New generation photovoltaics are gathering massive attention from the industrial and scientific community as a valid alternative to standard inorganic technologies thanks to the high efficiencies, suitability of printable deposition approach, low-cost and low-temperature processing[1-4]. The most impressive are the perovskite solar cells (PSCs) that have walked a milestone with a major report on high-performing PSCs passing from a power conversion efficiency (PCE) of 3.8% in 2009[5] arriving nowadays with leading efficiency of 25.7%[6, 7]. Perovskite semiconductors in photovoltaics are exploited in various permutable compositions due to their facile solution processible compositions, outstanding optoelectronic properties, and improvements in fabrication techniques[8-10]. The possibility to tune its bandgap permits it to be the perfect fit into tandem solar cells and overcome the single-junction theoretical efficiency limit[11]. The combination of PSCs as top cell with silicon bottom cell permits to achieve maximum PCE of 29.8% in monolithic configuration and similar efficiencies in different tandem configurations (mechanically stacked, 3T or 4T)[12-17]. Furthermore, PSCs have shown its superior power output at low-light conditions (200lux – 1000lux) compared with the commercial photovoltaics[18]. The low rate of non-radiative recombination allows to have high voltage output in indoor illumination, with the maximum PCE obtained of 40%, opening future applications for smart integration into low-powered electronics, such as sensors & IoT[19-22]. Despite high efficiencies of single-junction PSCs obtained on lab-scale and mini-module size (Active Area range = 10 – 100 cm^2)[23-27], stability under continuous working conditions (1 Sun) remains far behind that of the industrial Silicon devices[28]. While extrinsic degradation factors like moisture and oxygen, can be solved by proper sealing techniques, intrinsic phenomena due to illumination and heat such as ion migration, non-radiative recombination, and perovskite bulk decomposition remains a challenge forachieving a stable lifetime of nearly 10 years for a perovskite solar cell

(PSC)[29, 30]. Considering different architectures, n-i-p or standard structure usually has higher PCE compared to the p-i-n or the inverted structure, even if, lately, p-i-n devices are closing the gap with PCEs reaching up to 25%[6, 31-34]. In p-i-n architecture, insertion of additives into perovskite precursors is demonstrated as an effective approach to enhance efficiency and stability by passivating bulk and GBs defects[35]. In the past couple of years, ionic liquid, which was formerly introduced to n-i-p structure for its energy band alignment of the perovskite and the charge extraction layer[36], 1-butyl-3-methylimidazolium tetrafluoroborate (BMIMBF4) was adopted as an additive to the perovskite in p-i-n architecture leading to a more stable device with 20.0% efficiency[37]. In addition to the library of additive passivation in p-i-n architecture[38], the efficiency gap in comparison to n-i-p is improved using surface anchoring alkylamine ligands and an optimal amount of oleylamine (OAm) which proved to suppress nonradiative carrier recombination and showed 22.3% certified efficiency and no loss of efficiency for over 1000h in nitrogen atmosphere[39]. In 2021 Chen et al. addressed not only the stability of PSCs but the lifetime of precursor solutions for the fabrication of PSCs. Adding benzylhydrazine hydrochloride (BHC) the the perovskite ink reduces I_2 formation from I^- in solution and prenvent the I_2 formation in solid perovskite films during a light soaking stress test, improving the PCE to a certified efficiency of 22.62%[40]. In this work, taking note of the various passivation technique, we devised a strategy of combining those three additives to set a universal passivation approach for triple cation perovskites. In particular, we studied the effect of the triple additive doping on a narrow bandgap formulation (3C-NBg hereafter) and a wider bandgap perovskite (3C-WBg hereafter). We proposed the collective use of BMIMBF4 (IL), OAm, and BHC in the perovskite solution. These additives improved all the PV parameters which are ascribed to higher quality film, reduced non-radiative recombination, and allowed for a passivation of defects at the grain boundaries region. Upon inclusion of the additives, the 3C-NBg based PSC (Bg = 1.58eV)

shows a max PCE passing from 16.35% to 20.31%, mirroring the performance with 3C-WBg (Bg = 1.63eV) which shows a robust improvement in efficiency from 14.91% to 20.30%, with a FF of 83% and a PCE close to 30% in low-light condition. An impressive light stability improvement in air environment with a basic encapsulation (kapton tape) was observed for both the formulations. The additives enhanced more than 400% the time it takes for the maximum power point (MPP) trace to decay to 80% of the initial value[41] (T_{80}), reaching a T_{80} of 305h with the 3C-WBg. In addition, by changing the deposition technique of the electron transporting layer (ETL) from a solution process to an evaporated process the 3C-WBg shows a T_{80} that exceeds 1000h under continuous illumination. To demonstrate the universal approach of the additive combination, we tested them on a more stable formulation, such as a methylammonium-free double cation formulation (CsFA hereafter). An outstanding stability was reached by the additive doping arriving at T_{90} >1500h under continuous light stress in ambient air and a T_{80} > 6150h for thermal stress at 85°C. However, keeping in mind the applicability of wider bandgap perovskites in perovskite-silicon tandem cells, we checked our doped 3C-WBg with a semi-transparent ITO electrode and yielded a high-performing PCE of 15.5%. We demonstrate that this approach can be applied also for four terminal perovskite/silicon tandem to improve the overall efficiency of the cell.

Results and discussion

The choice of BMIMBF4, OAm and BHC as perovskite additives (Figure 1a) lies in the different ways they improve the quality of the perovskite absorber when they are added to the perovskite ink.[37, 39, 40] By acting on different aspects of the device passivation, we demonstrated that we can indeed combine them achieving a step-by-step improvement of the device performance (see Figure S1): IL helps improving Jsc and FF mainly, acting on the passivation of perovskite layer at the grain boundaries and to reduce the halide migation[39]. OAm improves the Voc, since it has been reported tocontrol of the crystal orientation, along with that minor passivation effects[42]. Finally, BHC boost J_{sc} and V_{oc} as well, preventing the formation of defect sites associated to the oxidation of I^- to I_2 [41].

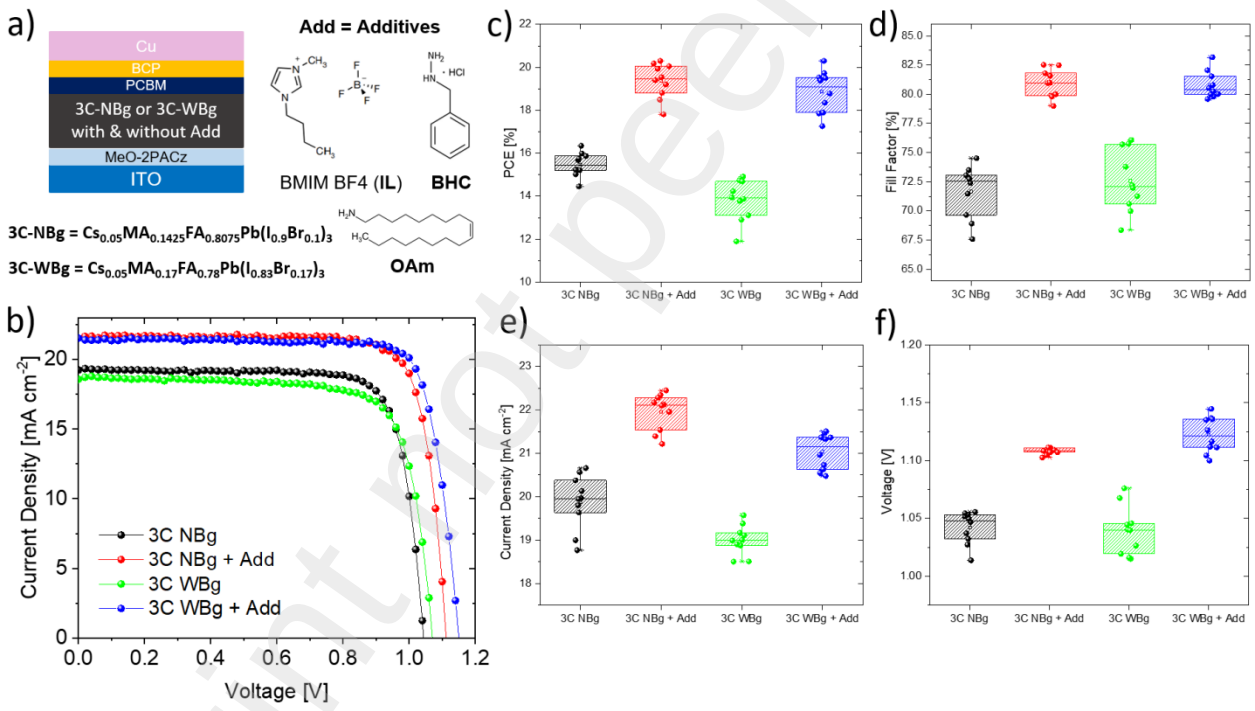

Figure 1 (a) Scheme of the device architecture used in this work, together with full device composition of narrow and wide band gap perovskite, named NBg and WBg respectively, and the 3 additives adopted, named Add, which includes 1-Butyl-3-methylimidazolium tetrafluoroborate (BMIM BF4 or IL), Benzylhydrazine hydrochloride (BHC) and Oleylamine (OAm); (b) current density as a function of voltage curve of the best device fabricated per type; electrical performance statistics of 10 devices per type fabricated, power conversion efficiency or PCE (c), fill factor (d), current density (e) and voltage (f) box plot comparison.

Table 1. Electrical parameters for the best devices and average on 10 samples ± standard deviation for each perovskite device type, extracted by the J–V curve acquired at 1 Sun irradiation.

Perovskite		PCE [%]	J_{sc} [mA cm^{-2}]	V_{oc} [V]	FF [%]	Integrated J_{sc} [mA cm^{-2}][a]
NBg	Best	16.35	20.66	1.05	78.47	20.48
	Average	15.45±0.55	19.95±0.62	1.04±0.01	72.56±4.53	
NBg + Add	Best	20.31	22.45	1.11	82.52	22.31
	Average	19.47±0.81	22.11±0.61	1.10±0.01	80.97±7.24	
WBg	Best	14.91	19.57	1.08	76.08	19.86
	Average	13.90±0.94	18.99±0.55	1.04±0.02	72.07±4.85	
WBg + Add	Best	20.30	21.51	1.14	83.17	21.74
	Average	19.08±0.98	21.14±0.72	1.12±0.02	80.39±2.39	

[a)] Integrated J_{sc} was obtained from the IPCE measurements of the best devices per type.

To prove the universal benefit of the additives in the perovskite, we used two perovskite formulations, one with a narrow band gap ($Cs_{0.05}MA_{0.14}FA_{0.81}Pb(I_{0.9}Br_{0.1})_3$, 3C-NBg, Eg~1.58eV) and one with wider band gap ($Cs_{0.05}MA_{0.17}FA_{0.77}Pb(I_{0.83}Br_{0.17})_3$, 3C-WBg, Eg~1.63eV); we implemented them in a perovskite solar device choosing the inverted structure, since it has been proven to be more robust and stable under stress conditions[38, 42, 43]. The main photovoltaic parameters of both perovskite precursors with and without additives are shown in Figure 1 and listed in Table 1: both NBg and WBg perovskite improves their PCE starting from 16.35% and 14.91% for pristine perovskite, up to 20.31% and 20.30% for perovskite with additives, respectively; all the PV parameters are improved, for both perovskites, with improved short circuit current density (J_{sc}), fill factor (FF) and open circuit voltage (V_{oc}), with an average PCE improvement by 25% and 37% on NBg and WBg, respectively. Integrated current density has been also measured from IPCE (see Table 1) and compared with J_{sc} obtained from J-V curves: all integrated J_{sc} values from IPCE are within a 2% deviation from to J_{sc} extracted from J-V curves, valiating the calibration procedure for the measurement at 1 Sun (Figure S2).

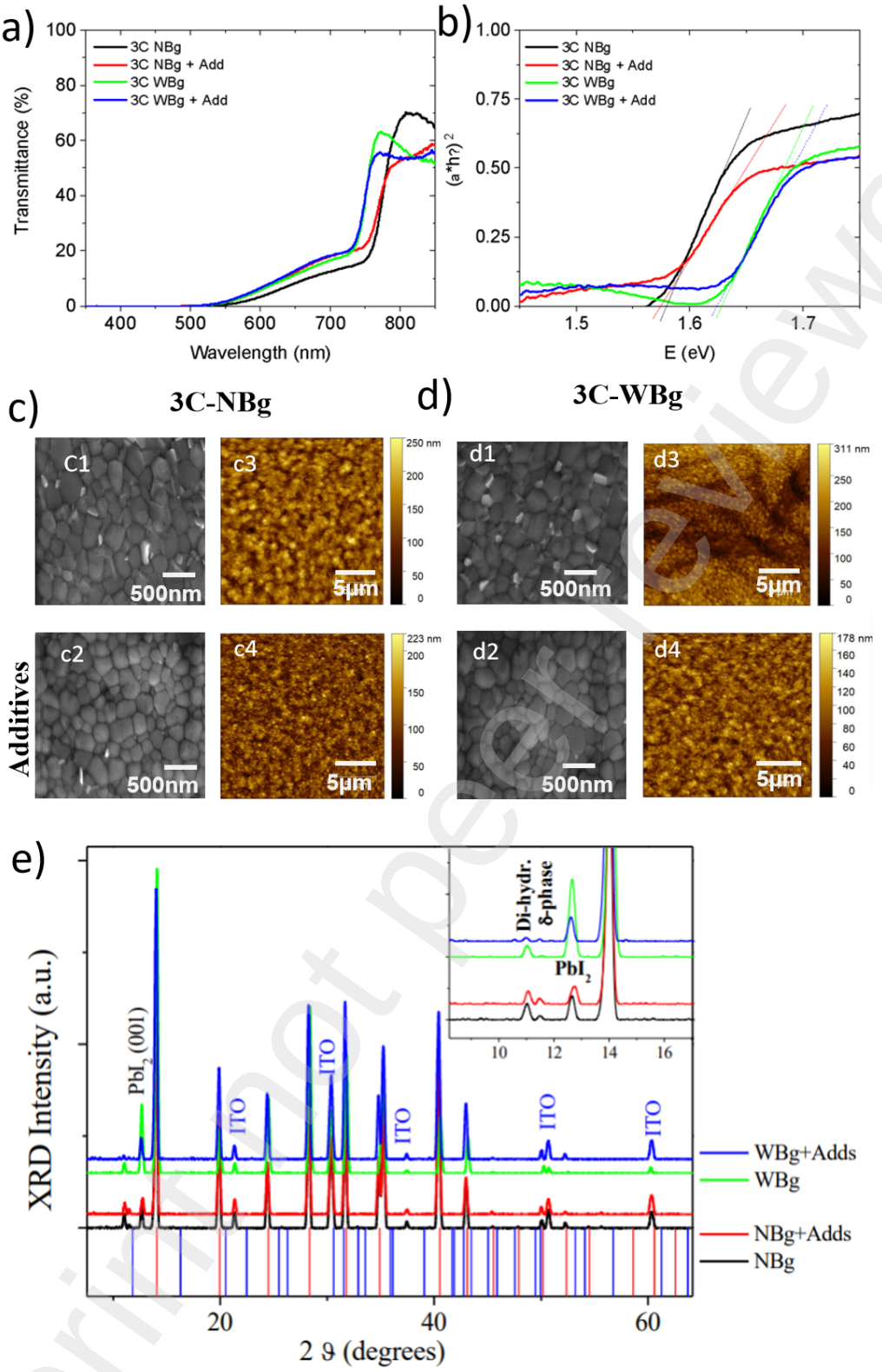

Figure 2. Analytical results on the triple cation (3C) films. The label NBg indicates the $Cs_{0.05}MA_{0.14}FA_{0.81}Pb(I_{0.9}Br_{0.1})_3$ formulation, while WBg indicates the $Cs_{0.05}MA_{0.17}FA_{0.77}Pb(I_{0.83}Br_{0.17})_3$ formulation. All the films are deposited on glass/ITO/MeO-2PACz substrates; (a) Transmittance (with integrating sphere) of the 3C perovskite films with and without the mixture of additives ; (b) Tauc plot the 3C perovskite films with and without additives used to identify the bandgap of the films; (c) SEM and AFM analysis of the NBg perovskite with (c2 and c4) and without additives (c1 and c3); (d) SEM and AFM analysis of the WBg perovskite with (d2 and d4) and without additives (d1 and d3); (e) XRD patterns of the 3C perovskites films with and without additives. Red and blue columns refer to theoretical alpha and delta perovskite phases respectively.

To investigate why the combination of additives induces such a drastic increase in the performance of our 3C-based PSC, we investigated how they affect the film morphology and the optoelectrical properties. The scope is to verify whether the miture of additives induce a change in the crystallization itself (i.e. lower amount of pinholes or larger grain size) or if they act mainly in the passivation of electronic defects reducing the losses due to non-radiative recombination.

In terms of the optical properties of the films, the introduction of the three additives in the 3C perovskite ink has only a minor effect. If one looks at the transmittance of the perovskite films deposited on glass/ITO/MeO-2PACz (see Figure 2a) the additives seem to slightly increase the transmittance below the bandgap. We believe that this effect is mainly due to the change in the roughness of the films as evidenced by the results of the AFM analysis (see Figure S4 and 2cd) and to the minor reduction of thickness induced by the addition of additives. Similarly, the additives have also a negligible effect on the bandgap of the films as measured from the Tauc plot (see Figure 2b), suggesting that they are not changing the crystalline structure of the perovskite films. On the other hand, the morphology of the films shows that the use of additives can prevent (or mitigate) the formation of grains of lead iodide as visible from the SEM images (see Figure 2c and Figure 2d). The images show a drastic decrease in the bright grains that are usually attributed to lead iodide cluster[44] (and confirmed by XRD), while the change in grain size appears negligible. This analysis is giving a first evidence of the positive effect of the additives used in this work, as they can improve the phase purity of the films. It is worth noting that both our 3C formulations (NBg and WBg) contain a 4% excess of the lead salts in the perovskite inks as largely reported in literature[45]. The disappearance of lead iodide clusters from the surface of the perovskites indicates that the additives are either preventing the crystallization of lead iodide only on the surface, or they are promoting a termination of the perovskite grains with an amorphous film of lead iodide, or they are blending in with the lead iodide to form a perovskite structure. While we cannot exclude the third option (the IL might be act as a large cation with a pseudohalide as anion) the quantities used (about 0.03 mol%) are too little to bond with all the lead iodide excess. For this reason, we believe the

additives are mainly changing the way the lead iodide grows in the crystals. The XRD patterns (Figure 2e) suggest that the effect of the additives on the crystalline phases are not too different for the two 3C formulations: in both cases we can observe a decrease in the peak of lead iodide (at 12.7°) suggesting that its crystallization is strongly reduced, while the perovskite peaks position are not shifting, suggesting that the additives are not altering the perovskite lattice and therefore are mainly located at grain boundaries[37]. Furthermore, the beneficial effect of the additives is also visible in the reduction of the peaks associated with hydrated perovskite phases showing that the passivation is also increasing the environmental stability of the films[46]. Such effect is even more evident for the WBg formulation with additives, which is also showing a strong decrease in the peaks associated with hydrated perovskite or the unwanted δ-phase. The presence of hydrated phases is due to the storage, transportation and measurement of all perovskite film under investigation that occurred in a non-controlled atmosphere. Anyhow, this additional stress is useful to identify better environmental stability of the films when the additives are used. The same stability is also enhanced by the increase in the Br content as previously reported, making our WBg perovskite more stable under shelf-life condition with respect to the NBg. Later we will also verify this effect by noticing that the WBg formulation can increase the stability of the complete devices under light soaking in ambient condition. So, from these data we can conclude that the additives are indeed changing the phase-composition of the film, making it purer and more resilient to humidity. To prove the enhanced structural stability induced by the additives in more controlled environment, we performed XRD analysis on aged 3C perovskite films stored in N_2 for 3000 h (Figure S3). In 3C WBg films, the perovskite structure is preserved, still being cubic alpha phase and no spurious contribution are detected. Quantitative analysis of crystallinity evinced that in the sample wituout additives PbI_2 contribution is ehnanced of 330% after storage, while its growth is reduced to only 50% in the case of doped film (Figure S3a). In 3C NBg compositions it is observed a change of crystallinity after more than 4 months of storage: in pristine samples , the crystallinity is reduced by 30%, while when additives are added the crystallinity reduction is contained to less than 20%, even

if a strong comparable increase of PbI_2 peak is observed in 3C NBg and 3C NBg + Add (Figure S3b). As discussed before, AFM analysis is showing that the mixture of additives decreases the roughness of the film (see Figure S4 and Figure 2cd). This is beneficial when the perovskite must be coated with a thin layer of PCBM as in our case, promoting the full coverage of the perovskite grains. All the changes induced by the additives on the morphology indicate an improvement in the film quality, but even the sum of these results might be not sufficient to justify the large improvement of PCE shown in Figure 1. To further delve into the additives' passivation effect, we measured the steady-state photoluminescence (PL) of the films (see Figure 3a). In this case, we can have direct evidence of the reduction of the non-radiative recombination, and indeed we can

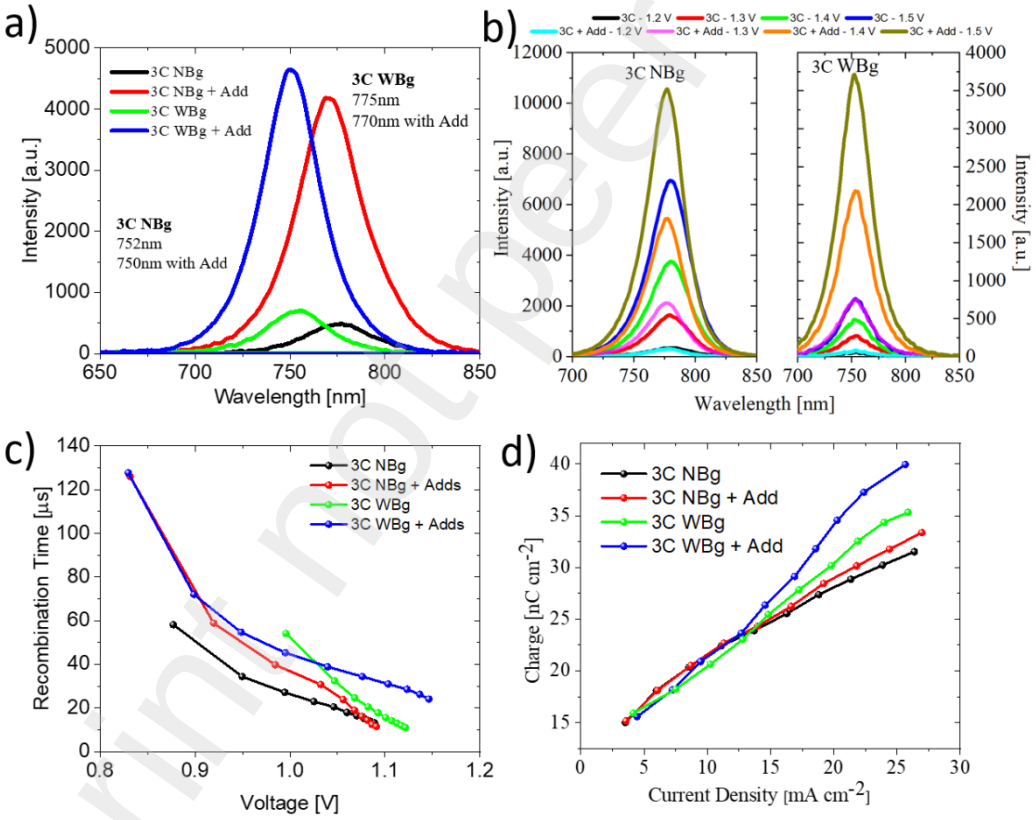

Figure 3. Optoelectronic properties of the triple cation (3C) films. The label NBg indicates the $Cs_{0.05}MA_{0.14}FA_{0.81}Pb(I_{0.9}Br_{0.1})_3$ formulation, while WBg indicates the $Cs_{0.05}MA_{0.17}FA_{0.77}Pb(I_{0.83}Br_{0.17})_3$ formulation; (a) steady state photoluminescence of the 3C films with and without additives deposited on glass/ITO/MeO-2PACz substrates; (b) electroluminescence of devices (with stack glass/ITO/MeO-2PACz/3C perovskite/PCBM/BCP/Cu) with and without additives. The forward bias value is indicated in the legend; (c) recombination time measured from fitting the transient photovoltage decay of devices (with stack glass/ITO/MeO-2PACz/3C perovskite/PCBM/BCP/Cu) with and without additives; (d) charge extraction measured from a fitting of the transient photovoltage decay of devices (with stack glass/ITO/MeO-2PACz/3C perovskite/PCBM/BCP/Cu) with and without additives.

observe how the additives induce a major increase in the PL: the PL signals increase by about an order of magnitude for both formulations, proving that the additives are indeed passivating the electronic defects in the films. The same behaviour can be seen also in the measurement of electroluminescence from full devices (see Figure 3b). These measurements show that the passivation is responsible for the V_{oc} increase of our devices. This is also confirmed by the transient photovoltage and photocurrent decay (TPV and TPC, see Figure 3cd): a longer recombination time means that the charges can travel for a longer time before recombining. We observed a clear enhancement of the recombination time (Figure 3c) when additives are included with respect to pristine samples. The enhancement of the recombination times at voltages close to the V_{oc} of our devices is also justifying the high FF that we measured. A similar behavior is observed for charge accumulation, with a slight increase at higher light intensity for TPC (Figure 3d) which means superior extraction efficacy and, therefore, less surface traps. According to the data presented here, we can conclude that the mixture of additives is providing a major passivation effect while also improving the phase purity of our films. The combination of these two effects justifies the large improvement in device performance.

As examples of the improvement iduced by the additives in a wide range of application , WBg + Add based perovskite devices have been further measured under indoor light (Figure 4ab) and in combination with a Silicon solar cell in a 4Terminal (4T) tandem configuration (Figure 4cd). At low light condition the Perovskite low rates of non-radiative recombination and short charge carrier lifetime permit to boost the maximum theoretically efficiencies above 50%[47]. This has been verified by suppressing trap states of the perovskite film with a decrease of nonradiative recombination leading to a Voc enhancement[19]. Here it is interesting to notice that 29.7% efficiency has been achieved at 1000lux passing from a 24.6% for undoped perovskite mainly due to a boost of Voc even at lower light intensity (Figure S6). The best device provides a maximum power output of 114.4 $\mu W*cm^{-2}$ with an incident light power of 385 $\mu W*cm^{-2}$, showing that this perovskite is able to work well at low light conditions, with a huge potentiality of its integration on low-powering

electronics to entering in the Internet of Things (IoT) world. For complementarity, a WBg + Add perovskite has been also measured as top cell with a standard commercially available Silicon heterojunction in a 4T configuration (inset of Figure 4c). In this case, Cu top electrode was replaced by sputtered ITO on top of BCP, achieving a maximum PCE of 15.5% for the semitransparent PSCs (Figure S7). In the 4T configuration, the semitransparent cell is used as an optical filter for the Si sub-cell, which decrease its efficiency from 20.8% to 8.2%. The overall combination of the two PCEs (semi-T PSC + filtered Si) lead to a final efficiency of 23.7% in tandem configuration (Figure S8), proving a boost in efficiency with respect to the single Si solar cell. It is worth noting that with further optimization of the transmittance of the perovskite cell above the bandgap will lead to further improvement of this structure. These applications are just few examples of the beneficial effect of IL, OAm and BHC in the perovskite, witnessing that such devices may easily go into the market delivering suitable output power for IoT devices and improving the current technology.

a)

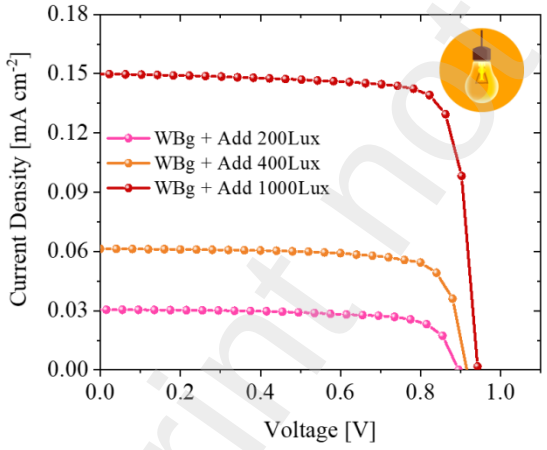

b)

	Voc [mV]	Jsc [μA cm^{-2}]	FF [%]	PCE [%]	Pout[μW cm^{-2}]
3C WBg+Add 200Lux	895	30.50	72.63	25.75	19.83
3C WBg+Add 400Lux	919	61.35	77.14	30.21	43.51
3C WBg+Add 1000Lux	949	147.08	78.15	28.34	109.10

c)

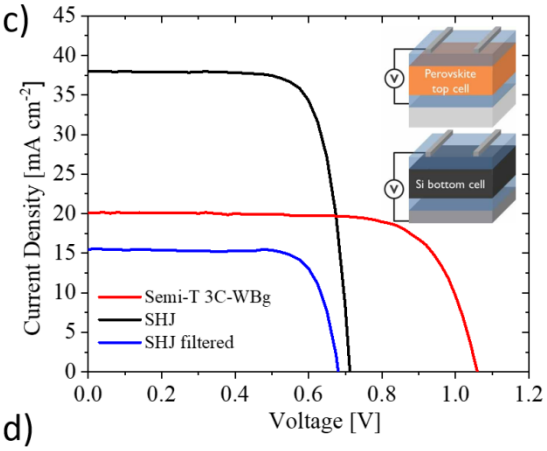

d)

	Voc [mV]	Jsc [mA cm^{-2}]	FF [%]	PCE [%]
Semi-T 3C-WBg	1060	20.1	73.0	15.5
SHJ	715	38.0	76.5	20.8
SHJ filtered	685	15.5	77.0	8.2
Total 4T tandem				23.7

Figure 4. J-V curves under different indoor illumination of a WBg + Add based perovskite (a), with thier corresponding photovoltaic parameters (b), and in combination with a Silicon device in a 4 terminal configurations (c), with their corresponding photovoltaic parameters (d).

To further prove the beneficial use of additives in perovskite solar cells, we investigated the device lifetime stability under light soaking and thermal stress, using the standard protocols ISOS L-1 and ISOS T-1[48], as shown in Figure 4. In this study we included a methylammonium-free perovskite (CsFA hereafter), having the following formulation $Cs_{0.17}FA_{0.83}Pb(I_{0.9}Br_{0.1})_3$; the choice to include such dual cation perovskite relies on the stronger intrinsic stability of its structure, due to the absence of the organic cation methylammonium, a volatile material that is known to be the first responsible of perovskite degradation, especially under light and thermal stress[32, 43, 49-51]. It is worth to mention that light and thermal stress were performed in air environment and sealing the PSCs by only kapton tape, which is only partially resistant to moisture and oxygen permeation[52]. This means

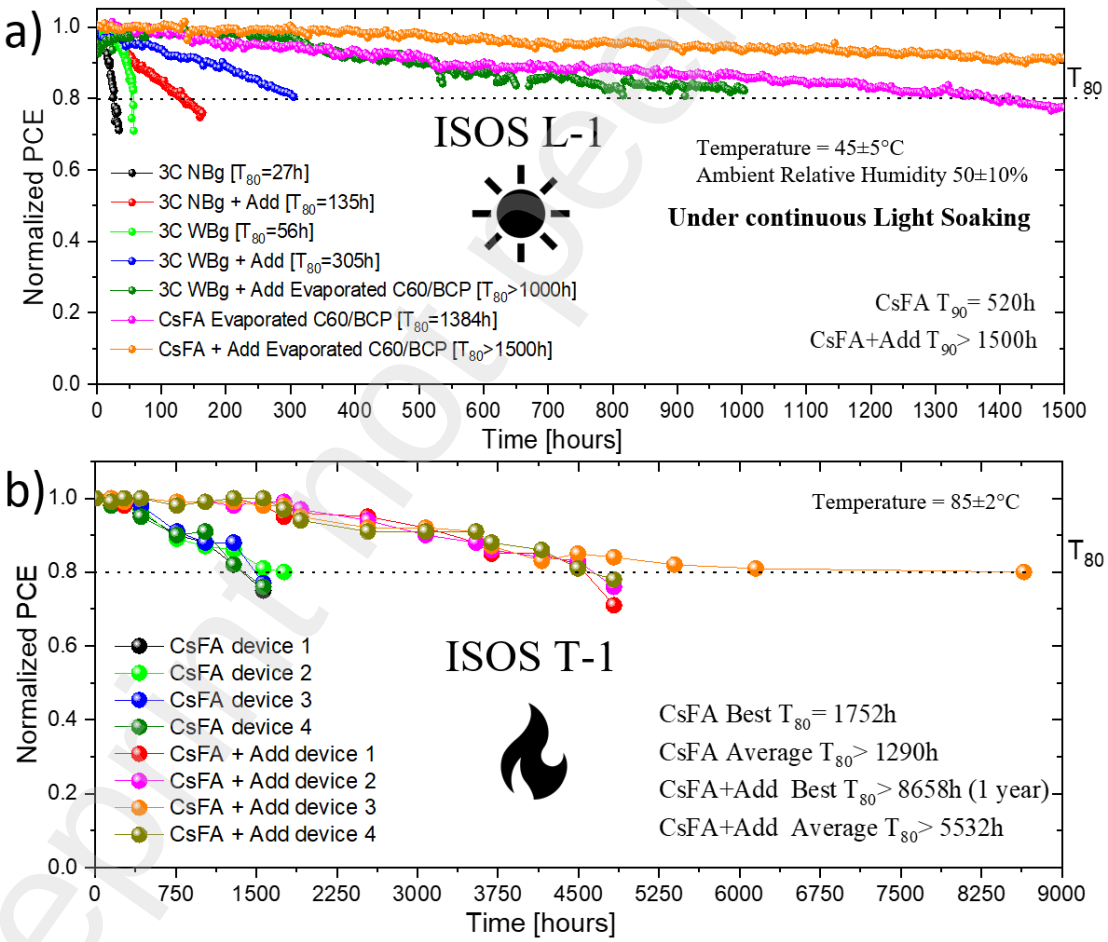

Figure 5. Stability test measurements following 2 of the most common standard tests used: ISOS L-1 (a), where the test has been taken under continuous light soaking in air condition; ISOS T-1 (b) where devices have been stored at 85°C in air environment and taken out only to measure the trend over time. Statistical data have been shown for ISOS T-1 (b), with up to 8 devices on CsFA perovskite with and without additives. All the devices monitored during light and thermal stress were sealed only by applying kapton tape.

than any improvemenet of the sstability can eb attributed to an enhancement of t bth intrinsic and extrinsic stability. The use of additives in the CsFA perovskite improves the photovoltaic parameters (see Figure S5) as well, confirming the wide application range of this perovskite "doping" process. NBg, WBg and CsFa with and without additives were compared first under continuous light soaking test (ISOS L-1). The T_{80}, the time in which 20% of the initial efficiency is lost, of NBg + Add, increases by ~ 400% compared to one of the pristine device without additives, passing from 27 to 135 hours; WBg + Add shown an improvement of the T_{80} by ~ 500% with respect to its pristine perovskite counterpart, passing from 56 to 305 hours; when using evaporated electron transport layer, such as C60/BCP, the improvement is further increased, showing a T_{80} over 1000 hours. Finally, a very remarkable stability is shown for the CsFA + Add perovskite device, with T_{90}, the time in which 10% of the initial efficiency is lost, improved by ~ 300% compared to pristine CsFA device, passing from 520 to over 1500 hours. Such results confirm that the use of additives improves the quality of different kind of perovskite device tested by limiting the degradation occurring under light soaking conditions. To further delve into the role of the addivie mix, a detailed assessment has been set it up for CsFA-based perovskite by adding the additives step by step (see Figure S9): the stability shows a T_{90} of 668, 1084, and 1528 hours, by using IL only, IL+OAm, and IL+OAm+BHC, respectively, proving that the higher stability is achieved by introducing the combination of the three additives.

To complete our stability assessment, we conducted a statistical thermal stress of CsFA-based devices: 4 devices per type (with and without additives) have been compared and labeled as device 1, 2, 3 and 4. A tremendous improvement is observed for CsFA thermal stability when we add the additives: T_{80} increases form 1290 hours of the CsFa till 5532 hous of the CsFA+Add (~ +428%). The best device reached an impressive T_{90} and T_{80} of 3540 and >8658 hours, respectively, corresponding to ~1 year. These results prove the potentiality of the use of these additives in any perovskite precursors to further stabilize their stability under continuous light soaking and thermal stress.

CONCLUSION

In conclusion, we have reported an universal approach for obtaining stable and highly efficient devices combining 3 different additives in the perovskite precursor ink: ionic liquids 1-Butyl-3-methylimidazolium tetrafluoroborate (BMIM-BF4), alkylamine ligands Oleylamine (OAm) and a reducing agent Benzylhydrazine hydrochloride (BHC). These additives improve the photovoltaic parameters with efficiencies passing from 16.35% to 20.31% for narrow band gap perovskite and from 14.91% to 20.30% to wide band gap perovskite, for pristine perovskite and perovskite with additives, respectively. Furthermore, we demonstrate the use of these additives in 2 main applications, for both indoor and tandem devices, delivering 29.7% and 23.7% efficiency under indoor (1000lux) and tandem configuration. Finally, the lifetime of the devices has been tested, choosing also a methylammonium-free perovskite, aiming to prove the universality of the perovskite passivation effect with the use of additives in the perovskite: tests under continuous light soaking and under 85°C (ISOS L-1 and ISOS T-1, respectively) showed impressive results, with T_{90} > 1500 hours and T_{80} > 8658 hours, respectively. In conclusion, this study provides a universal strategy to achieving high efficiency and stability in any perovskite precursor, with the goal of paving the road for the commercialization of perovskite solar technology.

Acknowledgments

L.A.C. and D.T. acknowledge funding from the Italian Ministry of Economic Development in the framework of the Operating Agreement with ENEA for Research on the Electric System. S.H.R. acknowledges “MAESTRO” project that received funding from the European Union’s Horizon 2020 research and innovation program under grant agreement number N° 764787. F.D.G acknowledges “Viperlab” project that received funding from the European Union’s Horizon 2020 research and innovation program under grant agreement number N° 101006715. The authors gratefully acknowledge the financial support of Regione Lazio through ISIS@MACH (IR approved by Giunta Regionale n. G10795, 7 August 2019 published by BURL n. 69 27 August 2019). A.D.C.

acknowledges the financial support of Mission Innovation grant between Italian Ministry of Ecological Transition and ENEA (agreement 21A033302 GU n. 133/5-6-2021). The authors are grateful to Marco Guaragno (CNR-ISM) for his technical support with X-ray experiments. L.A.C. and E.C. contributed equally to this work.

References

1. M.-E. Ragoussi and T. Torres, *Chemical Communications*, 2015, **51**, 3957-3972.
2. M. A. Green, 2006.
3. P. Gao, M. Grätzel and M. K. Nazeeruddin, *Energy & Environmental Science*, 2014, **7**, 2448-2463.
4. L. Schmidt-Mende, V. Dyakonov, S. Olthof, F. Ünlü, K. M. T. Lê, S. Mathur, A. D. Karabanov, D. C. Lupascu, L. M. Herz, A. Hinderhofer, F. Schreiber, A. Chernikov, D. A. Egger, O. Shargaieva, C. Cocchi, E. Unger, M. Saliba, M. M. Byranvand, M. Kroll, F. Nehm, K. Leo, A. Redinger, J. Höcker, T. Kirchartz, J. Warby, E. Gutierrez-Partida, D. Neher, M. Stolterfoht, U. Würfel, M. Unmüssig, J. Herterich, C. Baretzky, J. Mohanraj, M. Thelakkat, C. Maheu, W. Jaegermann, T. Mayer, J. Rieger, T. Fauster, D. Niesner, F. Yang, S. Albrecht, T. Riedl, A. Fakharuddin, M. Vasilopoulou, Y. Vaynzof, D. Moia, J. Maier, M. Franckevičius, V. Gulbinas, R. A. Kerner, L. Zhao, B. P. Rand, N. Glück, T. Bein, F. Matteocci, L. A. Castriotta, A. D. Carlo, M. Scheffler and C. Draxl, 2021, **9**, 109202.
5. A. Kojima, K. Teshima, Y. Shirai and T. Miyasaka, *Journal of the American Chemical Society*, 2009, **131**, 6050-6051.
6. M. Kim, J. Jeong, H. Lu, T. K. Lee, F. T. Eickemeyer, Y. Liu, I. W. Choi, S. J. Choi, Y. Jo, H.-B. Kim, S.-I. Mo, Y.-K. Kim, H. Lee, N. G. An, S. Cho, W. R. Tress, S. M. Zakeeruddin, A. Hagfeldt, J. Y. Kim, M. Grätzel and D. S. Kim, 2022, **375**, 302-306.
7. M. A. Green, E. D. Dunlop, J. Hohl-Ebinger, M. Yoshita, N. Kopidakis and X. Hao, 2021, **29**, 657-667.
8. J. S. Manser, J. A. Christians and P. V. Kamat, *Chemical Reviews*, 2016, **116**, 12956-13008.
9. N. J. Jeon, J. H. Noh, W. S. Yang, Y. C. Kim, S. Ryu, J. Seo and S. I. Seok, *Nature*, 2015, **517**, 476-480.
10. H. S. Jung and N.-G. Park, 2015, **11**, 10-25.
11. S. A. Kulkarni, T. Baikie, P. P. Boix, N. Yantara, N. Mathews and S. Mhaisalkar, *Journal of Materials Chemistry A*, 2014, **2**, 9221-9225.
12. J. Liu, M. D. Bastiani, E. Aydin, G. T. Harrison, Y. Gao, R. R. Pradhan, M. K. Eswaran, M. Mandal, W. Yan, A. Seitkhan, M. Babics, A. S. Subbiah, E. Ugur, F. Xu, L. Xu, M. Wang, A. u. Rehman, A. Razzaq, J. Kang, R. Azmi, A. A. Said, F. H. Isikgor, T. G. Allen, D. Andrienko, U. Schwingenschlögl, F. Laquai and S. D. Wolf, **0**, eabn8910.
13. E. Lamanna, F. Matteocci, E. Calabrò, L. Serenelli, E. Salza, L. Martini, F. Menchini, M. Izzi, A. Agresti, S. Pescetelli, S. Bellani, A. E. Del Río Castillo, F. Bonaccorso, M. Tucci and A. Di Carlo, *Joule*, 2020, **4**, 865-881.
14. J. Werner, B. Niesen and C. Ballif, 2018, **5**, 1700731.
15. G. Coletti, S. L. Luxembourg, L. J. Geerligs, V. Rosca, A. R. Burgers, Y. Wu, L. Okel, M. Kloos, F. J. K. Danzl, M. Najafi, D. Zhang, I. Dogan, V. Zardetto, F. Di Giacomo, J. Kroon, T. Aernouts, J. Hüpkes, C. H. Burgess, M. Creatore, R. Andriessen and S. Veenstra, *ACS Energy Letters*, 2020, **5**, 1676-1680.
16. B. Chen, Y. Bai, Z. Yu, T. Li, X. Zheng, Q. Dong, L. Shen, M. Boccard, A. Gruverman, Z. Holman and J. Huang, 2016, **6**, 1601128.
17. F. Gota, M. Langenhorst, R. Schmager, J. Lehr and U. W. Paetzold, *Joule*, 2020, **4**, 2387-2403.
18. K.-L. Wang, Y.-H. Zhou, Y.-H. Lou and Z.-K. Wang, *Chemical Science*, 2021, **12**, 11936-11954.
19. X. He, J. Chen, X. Ren, L. Zhang, Y. Liu, J. Feng, J. Fang, K. Zhao and S. Liu, 2021, **33**, 2100770.
20. S. Castro-Hermosa, G. Lucarelli, M. Top, M. Fahland, J. Fahlteich and T. M. Brown, *Cell Reports Physical Science*, 2020, **1**, 100045.
21. J. Xu, J. Xi, H. Dong, N. Ahn, Z. Zhu, J. Chen, P. Li, X. Zhu, J. Dai, Z. Hu, B. Jiao, X. Hou, J. Li and Z. Wu, *Nano Energy*, 2021, **88**, 106286.
22. D. Saranin, T. Komaricheva, L. Luchnikov, D. S. Muratov, T. S. Le, Y. Karpov, P. Gostishchev, S. Yurchuk, D. Kuznetsov, S. Didenko and A. Di Carlo, *Solar Energy Materials and Solar Cells*, 2021, **227**, 111095.
23. L. Vesce, M. Stefanelli, L. A. Castriotta, A. Hadipour, S. Lammar, B. Yang, J. Suo, T. Aernouts, A. Hagfeldt and A. Di Carlo, **n/a**, 2101095.

24. S. Chen, X. Dai, S. Xu, H. Jiao, L. Zhao and J. Huang, 2021, **373**, 902-907.
25. Y. Ding, B. Ding, H. Kanda, O. J. Usiobo, T. Gallet, Z. Yang, Y. Liu, H. Huang, J. Sheng, C. Liu, Y. Yang, V. I. E. Queloz, X. Zhang, J.-N. Audinot, A. Redinger, W. Dang, E. Mosconic, W. Luo, F. De Angelis, M. Wang, P. Dörflinger, M. Armer, V. Schmid, R. Wang, K. G. Brooks, J. Wu, V. Dyakonov, G. Yang, S. Dai, P. J. Dyson and M. K. Nazeeruddin, *Nature Nanotechnology*, 2022, **17**, 598-605.
26. Z. Li, T. R. Klein, D. H. Kim, M. Yang, J. J. Berry, M. F. A. M. van Hest and K. Zhu, *Nature Reviews Materials*, 2018, **3**, 18017.
27. M. Yang, D. H. Kim, T. R. Klein, Z. Li, M. O. Reese, B. J. Tremolet de Villers, J. J. Berry, M. F. A. M. van Hest and K. Zhu, *ACS Energy Letters*, 2018, **3**, 322-328.
28. D. Wang, M. Wright, N. K. Elumalai and A. Uddin, *Solar Energy Materials and Solar Cells*, 2016, **147**, 255-275.
29. C. C. Boyd, R. Cheacharoen, T. Leijtens and M. D. McGehee, *Chemical Reviews*, 2019, **119**, 3418-3451.
30. S. H. Reddy, F. Di Giacomo and A. Di Carlo, 2022, **12**, 2103534.
31. M. Stolterfoht, P. Caprioglio, C. M. Wolff, J. A. Márquez, J. Nordmann, S. Zhang, D. Rothhardt, U. Hörmann, Y. Amir, A. Redinger, L. Kegelmann, F. Zu, S. Albrecht, N. Koch, T. Kirchartz, M. Saliba, T. Unold and D. Neher, *Energy & Environmental Science*, 2019, **12**, 2778-2788.
32. S.-H. Turren-Cruz, A. Hagfeldt and M. Saliba, 2018, **362**, 449-453.
33. Z. Li, B. Li, X. Wu, S. A. Sheppard, S. Zhang, D. Gao, N. J. Long and Z. Zhu, 2022, **376**, 416-420.
34. Q. Jiang, J. Tong, Y. Xian, R. A. Kerner, S. P. Dunfield, C. Xiao, R. A. Scheidt, D. Kuciauskas, X. Wang, M. P. Hautzinger, R. Tirawat, M. C. Beard, D. P. Fenning, J. J. Berry, B. W. Larson, Y. Yan and K. Zhu, *Nature*, 2022, DOI: 10.1038/s41586-022-05268-x.
35. S. Liu, Y. Guan, Y. Sheng, Y. Hu, Y. Rong, A. Mei and H. Han, *Advanced Energy Materials*, 2020, **10**, 1902492.
36. J.-Y. Seo, T. Matsui, J. Luo, J.-P. Correa-Baena, F. Giordano, M. Saliba, K. Schenk, A. Ummadisingu, K. Domanski, M. Hadadian, A. Hagfeldt, S. M. Zakeeruddin, U. Steiner, M. Grätzel and A. Abate, *Advanced Energy Materials*, 2016, **6**, 1600767.
37. S. Bai, P. Da, C. Li, Z. Wang, Z. Yuan, F. Fu, M. Kawecki, X. Liu, N. Sakai, J. T.-W. Wang, S. Huettner, S. Buecheler, M. Fahlman, F. Gao and H. J. Snaith, *Nature*, 2019, **571**, 245-250.
38. T. J. Jacobsson, A. Hultqvist, A. García-Fernández, A. Anand, A. Al-Ashouri, A. Hagfeldt, A. Crovetto, A. Abate, A. G. Ricciardulli, A. Vijayan, A. Kulkarni, A. Y. Anderson, B. P. Darwich, B. Yang, B. L. Coles, C. A. R. Perini, C. Rehermann, D. Ramirez, D. Fairen-Jimenez, D. Di Girolamo, D. Jia, E. Avila, E. J. Juarez-Perez, F. Baumann, F. Mathies, G. S. A. González, G. Boschloo, G. Nasti, G. Paramasivam, G. Martínez-Denegri, H. Näsström, H. Michaels, H. Köbler, H. Wu, I. Benesperi, M. I. Dar, I. Bayrak Pehlivan, I. E. Gould, J. N. Vagott, J. Dagar, J. Kettle, J. Yang, J. Li, J. A. Smith, J. Pascual, J. J. Jerónimo-Rendón, J. F. Montoya, J.-P. Correa-Baena, J. Qiu, J. Wang, K. Sveinbjörnsson, K. Hirselandt, K. Dey, K. Frohna, L. Mathies, L. A. Castriotta, M. H. Aldamasy, M. Vasquez-Montoya, M. A. Ruiz-Preciado, M. A. Flatken, M. V. Khenkin, M. Grischek, M. Kedia, M. Saliba, M. Anaya, M. Veldhoen, N. Arora, O. Shargaieva, O. Maus, O. S. Game, O. Yudilevich, P. Fassl, Q. Zhou, R. Betancur, R. Munir, R. Patidar, S. D. Stranks, S. Alam, S. Kar, T. Unold, T. Abzieher, T. Edvinsson, T. W. David, U. W. Paetzold, W. Zia, W. Fu, W. Zuo, V. R. F. Schröder, W. Tress, X. Zhang, Y.-H. Chiang, Z. Iqbal, Z. Xie and E. Unger, *Nature Energy*, 2022, **7**, 107-115.
39. X. Zheng, Y. Hou, C. Bao, J. Yin, F. Yuan, Z. Huang, K. Song, J. Liu, J. Troughton, N. Gasparini, C. Zhou, Y. Lin, D.-J. Xue, B. Chen, A. K. Johnston, N. Wei, M. N. Hedhili, M. Wei, A. Y. Alsalloum, P. Maity, B. Turedi, C. Yang, D. Baran, T. D. Anthopoulos, Y. Han, Z.-H. Lu, O. F. Mohammed, F. Gao, E. H. Sargent and O. M. Bakr, *Nature Energy*, 2020, **5**, 131-140.
40. S. Chen, X. Xiao, H. Gu and J. Huang, 2021, **7**, eabe8130.
41. M. Saliba, M. Stolterfoht, C. M. Wolff, D. Neher and A. Abate, *Joule*, 2018, **2**, 1019-1024.
42. S. S. Mali and C. K. Hong, *Nanoscale*, 2016, **8**, 10528-10540.
43. L. A. Castriotta, R. Fuentes Pineda, V. Babu, P. Spinelli, B. Taheri, F. Matteocci, F. Brunetti, K. Wojciechowski and A. Di Carlo, *ACS Applied Materials & Interfaces*, 2021, **13**, 29576-29584.
44. M. Abdi-Jalebi, Z. Andaji-Garmaroudi, A. J. Pearson, G. Divitini, S. Cacovich, B. Philippe, H. Rensmo, C. Ducati, R. H. Friend and S. D. Stranks, *ACS Energy Letters*, 2018, **3**, 2671-2678.
45. B.-w. Park, N. Kedem, M. Kulbak, D. Y. Lee, W. S. Yang, N. J. Jeon, J. Seo, G. Kim, K. J. Kim, T. J. Shin, G. Hodes, D. Cahen and S. I. Seok, *Nature Communications*, 2018, **9**, 3301.
46. E. Calabrò, F. Matteocci, B. Paci, L. Cinà, L. Vesce, J. Barichello, A. Generosi, A. Reale and A. Di Carlo, *ACS Applied Materials & Interfaces*, 2020, **12**, 32536-32547.
47. I. Mathews, S. N. Kantareddy, T. Buonassisi and I. M. Peters, *Joule*, 2019, **3**, 1415-1426.
48. M. V. Khenkin, E. A. Katz, A. Abate, G. Bardizza, J. J. Berry, C. Brabec, F. Brunetti, V. Bulović, Q. Burlingame, A. Di Carlo, R. Cheacharoen, Y.-B. Cheng, A. Colsmann, S. Cros, K. Domanski, M. Dusza, C. J. Fell, S. R. Forrest, Y. Galagan, D. Di Girolamo, M. Grätzel, A. Hagfeldt, E. von Hauff, H. Hoppe, J. Kettle, H. Köbler, M. S. Leite, S. Liu, Y.-L. Loo, J. M. Luther, C.-Q. Ma, M. Madsen, M. Manceau, M. Matheron, M. McGehee, R. Meitzner, M. K. Nazeeruddin, A. F. Nogueira, Ç. Odabaşı, A. Osherov, N.-G. Park, M. O. Reese, F. De Rossi, M. Saliba, U. S. Schubert, H. J. Snaith, S. D. Stranks, W. Tress, P. A. Troshin, V. Turkovic, S.

Veenstra, I. Visoly-Fisher, A. Walsh, T. Watson, H. Xie, R. Yıldırım, S. M. Zakeeruddin, K. Zhu and M. Lira-Cantu, *Nature Energy*, 2020, **5**, 35-49.
49. X.-X. Gao, W. Luo, Y. Zhang, R. Hu, B. Zhang, A. Züttel, Y. Feng and M. K. Nazeeruddin, 2020, **32**, 1905502.
50. L. A. Castriotta, F. Matteocci, L. Vesce, L. Cinà, A. Agresti, S. Pescetelli, A. Ronconi, M. Löffler, M. M. Stylianakis, F. Di Giacomo, P. Mariani, M. Stefanelli, E. M. Speller, A. Alfano, B. Paci, A. Generosi, F. Di Fonzo, A. Petrozza, B. Rellinghaus, E. Kymakis and A. Di Carlo, *ACS Applied Materials & Interfaces*, 2021, **13**, 11741-11754.
51. L. A. Castriotta, R. Infantino, L. Vesce, M. Stefanelli, A. Dessì, C. Coppola, M. Calamante, G. Reginato, A. Mordini, A. Sinicropi, A. Di Carlo and L. Zani, **n/a**, e12455.
52. B. Li, M. Wang, R. Subair, G. Cao and J. Tian, *The Journal of Physical Chemistry C*, 2018, **122**, 25260-25267.

Table of Contents figure

An Universal Multi-Additive Strategy to Enhance Efficiency and Stability in Inverted Perovskite Solar Cells

Luigi Angelo Castriotta[1,#], Emanuele Calabrò[1,2,#], Francesco Di Giacomo[1], Sathy Harshavardhan Reddy[1], Daimiota Takhellambam[1], Barbara Paci[3], Amanda Generosi[3], Luca Serenelli[4], Francesca Menchini[4], Luca Martini[4], Mario Tucci[4], Aldo Di Carlo[1,3]*

ToC figure

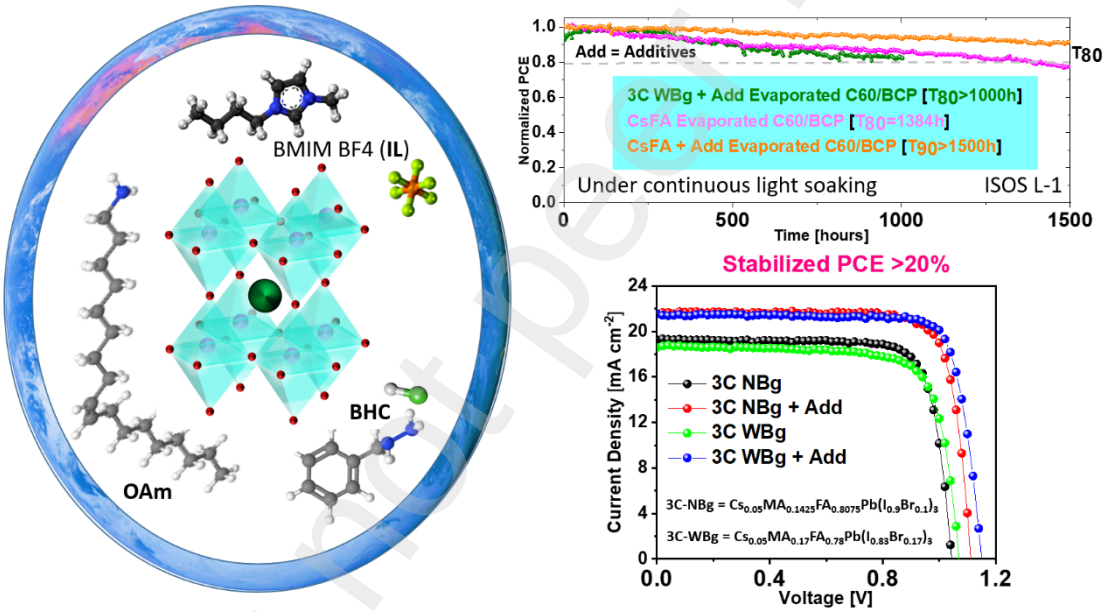

- A universal approach to enhance both performances and stability of inverted PSCs by introducing a combination of three additives.
- 3 types of Perovskite tested, improving their performances from 14.9% up to 20.31% efficiency.
- ISOS L-1 and ISOS T-1 reached a T_{90} > 1500 hours and a T_{80} > 8650 hours, respectively.